

A Robust RBF-ANN Model to Predict the Hot Deformation Flow Curves of API X65 Pipeline Steel

M. Rakhshkhorshid*

Department of Mechanical Engineering, Birjand University of Technology, POBOX 97175-569, Birjand, Iran

Abstract: In this research, a radial basis function artificial neural network (RBF-ANN) model was developed to predict the hot deformation flow curves of API X65 pipeline steel. The results of the developed model were compared with the results of a new phenomenological model that has recently been developed based on a power function of Zener-Hollomon parameter and a third order polynomial function of strain power m (m is a constant). Root mean square error (RMSE) criterion was used to assess the prediction performance of the investigated models. According to the results obtained, it was shown that the RBF-ANN model has a better performance than that of the investigated phenomenological model. Very low *RMSE* value of 0.41 MPa was obtained for RBF-ANN model, which was less than one-tenth of the *RMSE* value of 4.74 MPa obtained for the investigated constitutive equation. The results can be further used in mathematical simulation of hot metal forming processes.

Keywords: Hot deformation, Neural Computing, Radial Basis Function, Constitutive equations, Flow stress.

1. Introduction

Careful modeling of the flow curves of different materials at elevated temperatures is the first step in mathematical simulation of hot deformation processes such as hot rolling and hot forging. Thus, many research have been conducted to model the flow curves of different materials [1-4]. A critical review on these efforts can be found in Ref. [5]. Phenomenological, physical-based and artificial neural network (ANN) models are the main procedures that have ever been used for flow stress modeling [5]. In phenomenological constitutive models, regression analysis is used to adjust the constants of a predefined mathematical function so as to fit it over the experimental flow curves. Johnson- Cook [1], Arrhenius equation with strain dependent constants [6, 7] and exponential one with strain dependent constants [8] are some examples of this category. In contrast, physical-based constitutive models are the ones which consider the mechanisms of deformation such as dislocation dynamics, thermal activation and so on. Zerilli-Armstrong [9] Voyiadjis-Almasri [10] and a two-stage constitutive model developed based on the classical stress-dislocation relation and the kinetics of dynamic recrystallization [11] are some examples of physical-based models. The latter model has been used to model the hot deformation flow curves of 42CrMo steel [11] and a typical nickel-based superalloy [12]. Recently, artificial neural network, have widely been used in different scopes of engineering applications [13], as well as, in hot deformation flow curves modeling. The higher accuracy of ANN models over the constitutive models such as Arrhenius, Johnson-Cook (JC) and modified Zerilli- Armstrong (ZA) models for modeling the flow curves of an Al/Mg based composite has been shown by Senthilkumar et al. [14]. Based on the experimental results obtained from isothermal compression testing, Zhu et al. [15] developed an ANN model with a back-propagation learning algorithm to predict the flow curves of as-cast TC21 titanium alloy. They showed the higher prediction performance of the developed ANN model over a regression method. Mirzadeh et al. [16] developed a feed-forward ANN model to predict the flow curves of different steel types including 17-4 PH martensitic precipitation hardening stainless, a medium carbon microalloyed and a 304 H austenitic

Received by the editors July 13, 2016; Revised October 14, 2016 and Accepted November 22, 2016.

*Corresponding author (rakhshkhorshid@birjandut.ac.ir)

stainless steel. They compared the results of the developed ANN model with the results of the hyperbolic sine equation with strain dependent constants and a constitutive equation with simple normalized stress-normalized strain form. They found the ANN model as the best technique for modeling the available flow curves [17]. These, together with the other associated published works [17-22] show the ability of ANN techniques to model the hot deformation flow curves of different materials.

In this study, a radial basis function artificial neural network (RBF-ANN) model is used to predict the hot deformation flow curves of API X65 pipeline steel. The results of the developed RBF-ANN model are compared with the results of a new simple phenomenological model that has recently been developed based on a power function of Zener-Hollomon parameter and a third order polynomial function of strain power m (m is a constant) [23, 24]. The tested steel is a high strength low-alloy (HSLA) one that is used in Iran high-pressure gas transportation pipelines [25]. The chemical and mechanical specifications of this steel are characterized by API standard code [26].

2. Experimental Procedure

2.1. The experimental flow curves

The experimental flow curves of API X65 pipeline steel, obtained from hot compression tests at different temperatures and strain rates (as shown in Fig. 1 [25]) were used to develop a radial basis function artificial neural network (RBF-ANN) model to predict the hot deformation flow curves of tested steel. The details of the tensile testing equipment and conditions have been reported in Ref. [25]. As can be seen in most deformation conditions, the flow stress increases to a peak value and then gradually falls to a steady state stress that is the common pattern of dynamic recrystallization (DRX) occurrence. Though, for the most severe deformation condition with the temperature of 950 °C and the strain rate of 1 s⁻¹, true stress–true strain curve shows a typical dynamic recovery (DRV) behavior [25].

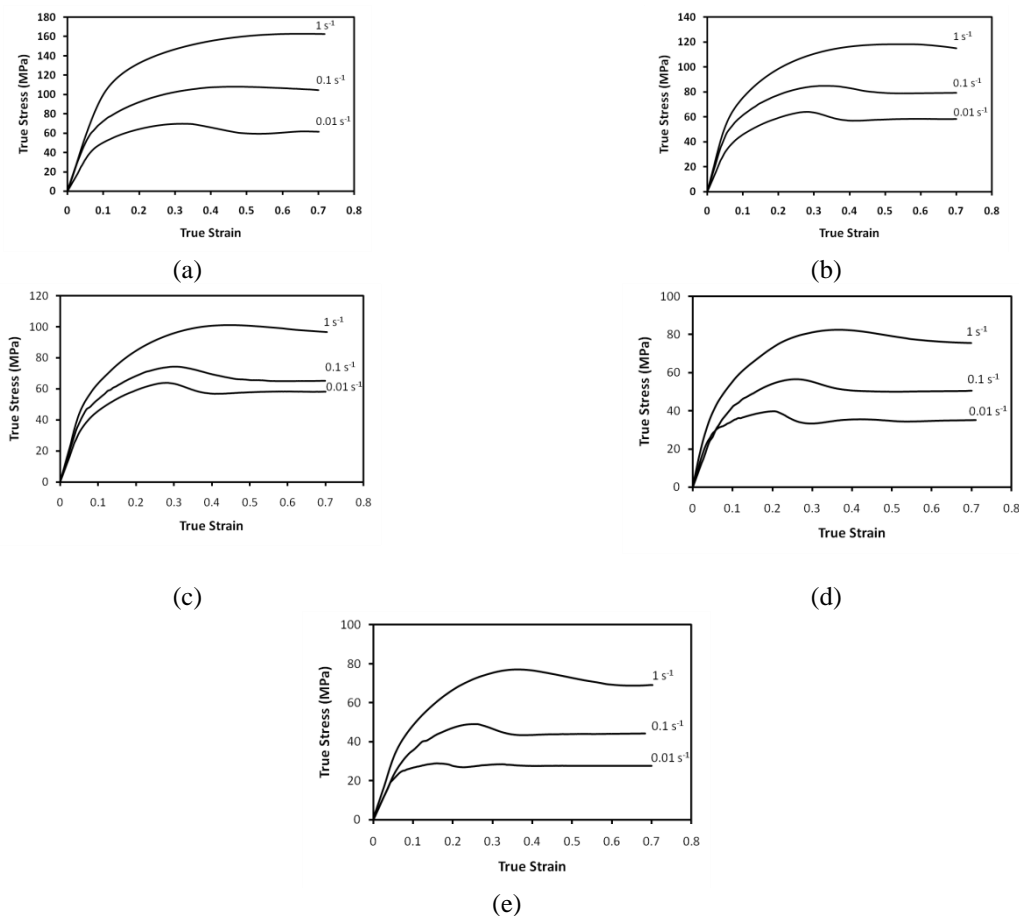


Fig. 1. Experimental flow curves of API X65 pipeline steel at different temperatures of (a) 950, (b) 1000, (c) 1050 (d) 1100 and (e) 1150 °C with different strain rates[25].

2.2. Radial basis function artificial neural network

A RBF-ANN was developed to predict the hot deformation flow curves of API X65 steel. Also, the results of the developed RBF-ANN were presented and compared with the results of the newly developed phenomenological equation published in Ref. [23].

2.2.1. The structure of the radial basis function artificial neural network

An ANN is composed of a large number of highly interconnected processing elements, called neurons, working together to solve a specific problem [27]. The radial basis function artificial neural networks are three layer networks usually with a Gaussian transfer function in the hidden layer and a linear transfer function in the output layer. The structure of the radial basis function artificial neural network applied in this research is depicted in Fig. 2.

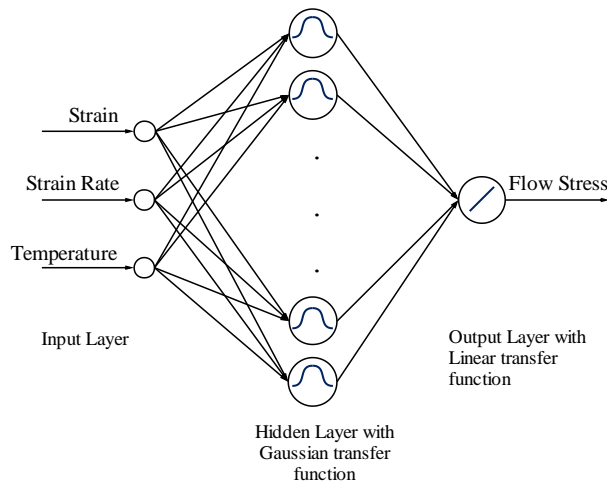


Fig. 2. The structure of the radial basis function artificial neural network, applied in the current work.

As explained elsewhere [28-30], in the RBF_ANNs, the input vectors are fed into the first layer of the network. The hidden layer is the second layer of RBF_ANNs that is composed of a set of neurons with Gaussian transfer function to measure the Euclidean distance between the centers of the hidden layer (μ_k ; $k = 1$ to L) and the input vector (x_i ; $i = 1$ to N). Hence, the output of the hidden layer neurons is calculated from:

$$v_k(x) = \exp\left(-\frac{\|x - \mu_k\|^2}{\sigma_k^2}\right) \quad (1)$$

where $\|x - \mu_k\|$ is the Euclidean distance between the k th center of the hidden layer and the input vector of x and is calculated from $\|x - \mu_k\| = \sqrt{\sum_{i=1}^N (x_i - \mu_k)^2}$, where σ_k is the spread of the k th neuron of the hidden layer and controls the sensitivity of it to the Euclidean distance. The third layer of the RBF_ANNs is the output layer. Usually, a linear transfer function is used in this layer that returns the value passed to it. Thus, the output of a RBF_ANN with a single output variable is equal to the weighted sum of the outputs of the hidden layer:

$$y = \sum_{k=1}^L w_k v_k(x) \quad (2)$$

where, w_k is the connecting weight of the k th neuron of the hidden layer to the output variable of the network (y).

2.2.2. Data base

The experimental stress-true strain curves obtained at different deformation temperatures and strain rates [25] were sampled for the different strains in the range of 0.1 to 0.7 with the step size of 0.01. Thus, a data base with the input variables of the deformation temperature, strain rate, strain and the output variable of

flow stress with 990 patterns was prepared. The prepared data base was divided into two subsets of training and testing. Two thirds of the overall data (i.e. 660 randomly selected patterns) was used for training and the rest was used for testing the generalization property of the developed neural network.

2.2.3. Neural network training and testing

After the construction of the neural network structure, a training algorithm is used to adjust the weights of the network so as to minimize the network mean square error (MSE) between the measured and predicted values of the output variable of the network, iteratively [28]:

$$MSE = \frac{1}{n} \sum_{i=1}^n (t_i - y_i)^2 \quad (3)$$

Where t_i and y_i are the target (actual) and predicted values of i th pattern of the output variable y , respectively and n is the number of data patterns used for training the network.

Data normalization is one important way to improve the prediction performance of the neural networks. Especially, when the ranges of input variables are in different magnitudes, this is a necessary [31]. In the current study, the input variables were normalized by transformation to a new data set, with a zero mean and a unit variance (using “mapstd” function of MATLAB platform) [32]. In RBF-ANNs, the number of neurons in the hidden layer and the spread value are the main factors influence the prediction performance of the developed network [33]. The number of the neurons in the hidden layer can be simply considered equal to the number of training patterns. Thus, the error between the predicted and measured (actual) network outputs for the training subset can be equal to zero; but, the generalization property of the trained network may be lost. In this work, after some trial and error the number of neurons in the hidden layer was set to 160. It was found that the higher number of neurons causes not to improve in the performance of the developed network for training data but lowers the prediction performance of the trained network for testing (unseen) subset. The $RMSE$ criterion was used to assess the prediction performance of the developed networks:

$$RMSE = \sqrt{\frac{1}{n} \sum_{i=1}^n (t_i - y_i)^2} \quad (4)$$

Where t_i is the target output, y_i is the model output and n is the number of overall data patterns. Furthermore, in the designing process of RBF-ANNs, it is needed to determine a proper spread value σ to control the sensitivity of hidden neurons [29]. In the other words, there is an optimum value for σ that after it, the performance of the developed RBF-ANN for the training data improves but decreases for the testing data. Here, to find the optimum value of spread (σ), different networks with different values of spread were trained and tested. The obtained results for training and testing patterns are shown in Fig. 3.

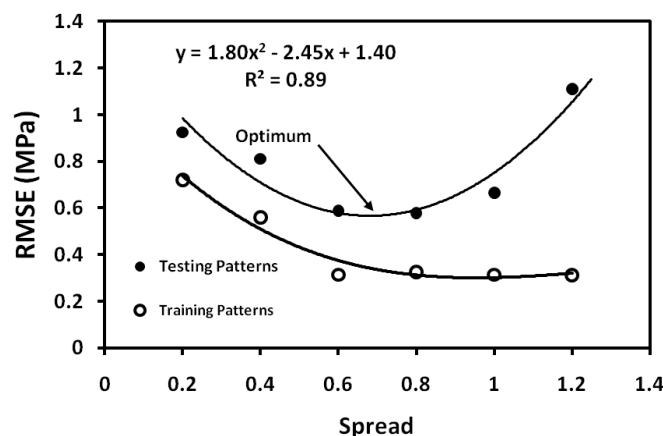


Fig. 3. The results ($RMSE$ values) obtained for training and testing patterns with different values of spread.

As can be seen, after the spread value of about 0.6 the developed model undergoes an over-fitting (i.e. no significant improve can be observed for training patterns; while, the *RMSE* value increases for testing patterns). As depicted, using the regression analysis, a second order polynomial function was fitted to the *RMSE* values obtained at different spreads for the testing data. The derivative of this polynomial function was set equal to zero to find an optimum spread value. Consequently, an optimized RBF-ANN, with the spread value of about 0.7 was obtained that was used to predict the hot deformation flow curves of API X65 pipeline steel.

2.2.4. Results of the developed neural network

The results of the developed RBF-ANN model with the spread value of 0.7 for training, testing and overall data patterns, in the shape of scatter diagrams, are presented in Fig. 4. As can be seen, there is an excellent agreement (with correlation coefficient value of $R = 0.9999$ for overall data) between the predicted and measured flow stresses. Furthermore, the low *RMSE* values of 0.31, 0.56, 0.41 MPa that were respectively obtained for training, testing and the overall data is the other evidence of this excellent agreement.

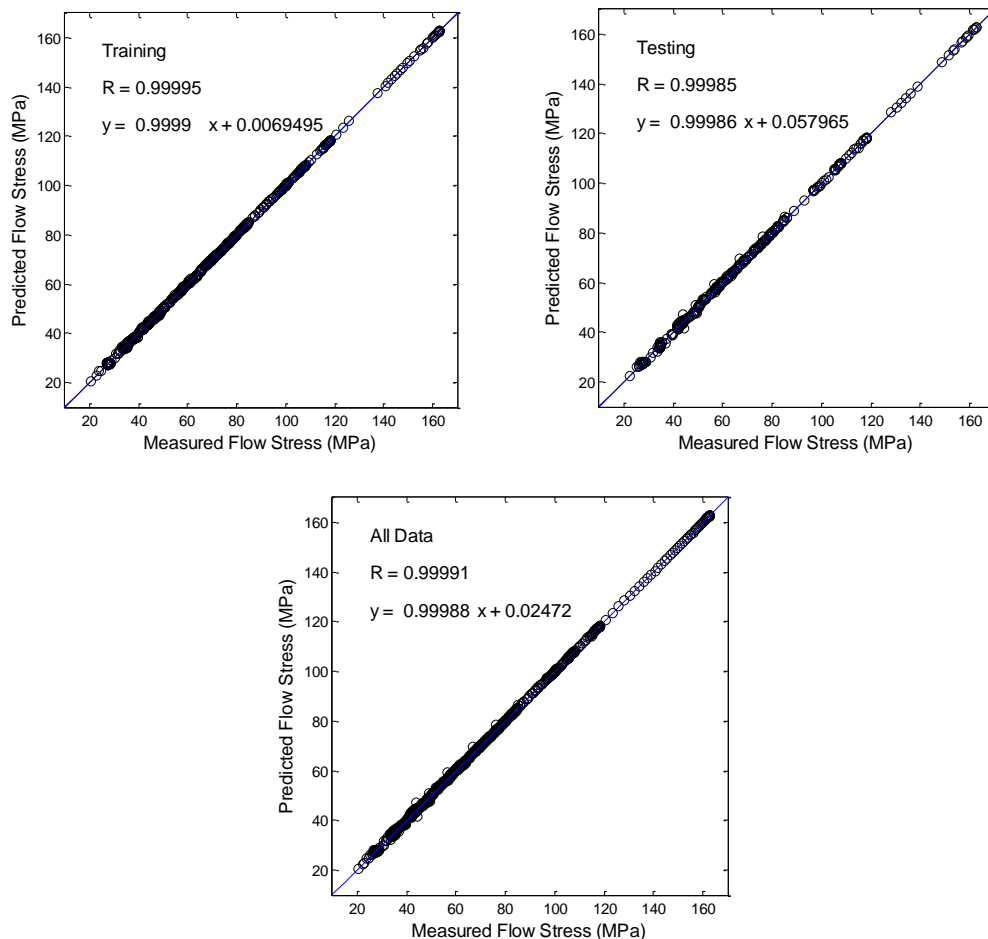


Fig. 4. The results of the developed RBF-ANN model with the spread value of 0.7 for training, testing and overall data patterns.

A comparison between the experimental and predicted flow curves (using the developed RBF-ANN model) at deformation conditions with two temperatures of 1000 and 1100 °C with different strain rates is presented in Figs. 5a and 5b, respectively. As can be seen, there is an excellent fit between the RBF-ANN simulated and experimental flow curves that is the evidence of robustness of the developed RBF-ANN model.

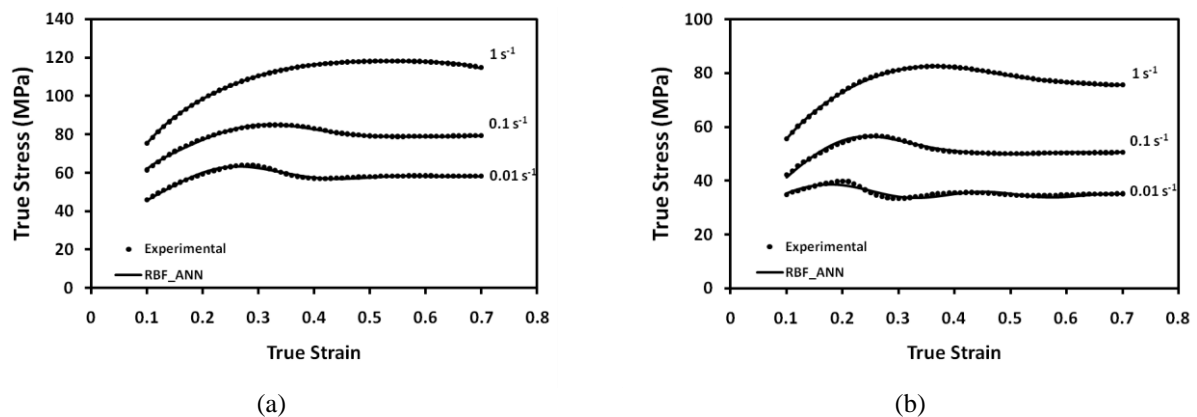


Fig. 5. The comparison between the experimental and modeled flow curves (using the RBF-ANN model) at deformation conditions with two temperatures of (a) 1000 and (b) 1100 °C with different strain rates.

2.3. Comparison of the results of the developed RBF-ANN model with the results of the investigated phenomenological model

The under studied phenomenological model has been developed previously by the author [23] and was used to describe the hot deformation flow curves of API X65 pipeline steel. Using the equation developed based on a power function of Zener-Hollomon parameter and a third order polynomial function of strain power a constant number the hot flow stress of API X65 pipeline steel can be expressed as follows [23]:

$$\sigma = \dot{\varepsilon}^{0.169} \exp\left(\frac{0.169 \times 346238}{RT}\right) \times (-0.006 + 2.420\varepsilon^{0.7} - 3.899\varepsilon^{1.4} + 2.046\varepsilon^{2.1}) \quad (5)$$

More details about finding the constants of this equation can be found in Refs. [23 and 24]. *RMSE* criterion was used to evaluate the prediction performances of the developed RBF-ANN model and investigated phenomenological model. According to the obtained results, it was found that the developed RBF-ANN model, with the *RMSE* value of 0.41 MPa, has a better performance than that of the investigated phenomenological constitutive equation. The obtained *RMSE* value for the developed RBF-ANN model was less than one-tenth of the *RMSE* value of 4.74 MPa [23] obtained for the investigated constitutive equation.

3. Conclusion

In this work, a RBF-ANN model was developed to predict the hot deformation flow curves of API X65 pipeline steel. The flow curves obtained from single hit compression testing at different deformation conditions were sampled. Consequently, a database with the input variables of deformation temperature, strain rate, strain and the output variable of flow stress was obtained. Accordingly, a RBF-ANN model was developed to model the hot deformation flow curves of tested steel. The prediction performance of the developed network was assessed and compared with the results of a recently developed constitutive equation, through the use of *RMSE* criterion. It was found that developed RBF-ANN model has better performance than that of the investigated constitutive equation (lower *RMSE*). Moreover, it was shown that using the developed RBF-ANN model, there is an excellent fit between the predicted and experimental flow curves (with correlation coefficient value of $R = 0.9999$ for overall data). This, together with very low *RMSE* value of 0.41 MPa obtained for overall data showed the robustness of the developed RBF-ANN model to predict the hot deformation flow curves of the tested steel in the temperature range of 950 to 1150°C and the strains between 0.01 to 1 s^{-1} .

4. References

- [1] G.R. Johnson and W.H. Cook, "A constitutive model and data for metals subjected to large strains, high strain rates and high temperatures. *In: Proceedings of the 7th international symposium on ballistics*, (1983) 541–543.
- [2] E. Voce, The relationship between stress and strain for homogeneous deformation. *J. Inst. Met.*, 74 (1948) 537–562.
- [3] A.S. Khan and S. Huang, Experimental and theoretical study of mechanical behavior of 1100 aluminum in the strain rate range 10^{-5} – 10^4 s⁻¹, *Int. J. Plast.*, 8 (1992) 397–424.
- [4] H. Mirzadeh and A. Najafizadeh, Flow stress prediction at hot working conditions, *Mater. Sci. Eng. A*, 527(2010) 1160–1164.
- [5] Y.C. Lin and X.M. Chen, A critical review of experimental results and constitutive descriptions for metals and alloys in hot working, *Mater. Des.*, 32 (2011) 1733–1759.
- [6] H. Shi, A.J. McLaren, C.M. Sellars, R. Shahani and R. Bolingbroke, Constitutive equations for high temperature flow stress of aluminium alloys, *J. Mater. Sci. Technol.*, 13 (1997) 210–216.
- [7] Y.C. Lin, M.S. Chen and J. Zhang, Constitutive modeling for elevated temperature flow behavior of 42CrMo steel, *Comput Mater Sci*, 424 (2008) 470–477.
- [8] M.Y. Zhan, Z. Chen, H. Zhang and W. Xia, Flow stress behavior of porous FVS0812 aluminum alloy during hot-compression, *Mech. Res. Commun.*, 33 (2006) 508–514.
- [9] P.J. Zerilli and R.W. Armstrong, Dislocation-mechanics-based constitutive relations for material dynamics calculations, *J. Appl. Phys.*, 61 (1987) 1816–1825.
- [10] G.Z. Voyiadjis and A.H. Almasri, A physically based constitutive model for FCC metals with applications to dynamic hardness, *Mech. Mater.*, 40 (2008) 549–563.
- [11] Y.C. Lin, M.S. Chen and J. Zhang, Prediction of 42CrMo steel flow stress at high temperature and strain rate, *Mech. Res. Commun.*, 35 (2008) 142–50.
- [12] Y.C. Lin, X.M. Chen, D.X. Wen and M.S. Chen, A physically-based constitutive model for a typical nickel-based superalloy, *Comput. Mater. Sci.*, 83(2014) 282–289.
- [13] M. Rakhshkhorshid and S.A. TeimouriSendesi, Bayesian Regularization Neural Networks for Prediction of Austenite Formation Temperatures (Ac1 and Ac3), *J. Iron Steel Res. Int.*, 21(2) (2014) 246 – 251.
- [14] V. Senthilkumar and A. Balaji, D. Arulkirubakaran, Application of constitutive and neural network models for prediction of high temperature flow behavior of Al/Mg based nanocomposite, *Trans. Nonferrous Met. Soc. China*, 23 (2013) 1737–1750.
- [15] Y. Zhu, W. Zeng, Y. Sun, F. Feng and Y. Zhou, Artificial neural network approach to predict the flow stress in the isothermal compression of as-cast TC21 titanium alloy, *Comp. Mater. Sci.*, 50 (2011) 1785– 1790.
- [16] H. Mirzadeh, J.M. Cabrera, J.M. Prado and A. Najafizadeh, Modeling and prediction of hot deformation flow curves, *Metall. Mater. Trans. A*, 43 (2012) 108–123.
- [17] N. Haghdadi, A. Zarei-Hanzaki, A.R. Khaledian and H.R. Abedi, Artificial neural network modeling to predict the hot deformation behavior of an A356 aluminum alloy, *Mater. Des.*, 49 (2013) 386–391.
- [18] Y.C. Lin, X. Fang and Y.P. Wang, Prediction of metadynamic softening in a multi-pass hot deformed low alloy steel using artificial neural network, *Mater. Sci.*, 43 (2008) 5508–5515.
- [19] N.S. Reddy, Y.H. Lee, C.H. Park and C.S. Lee, Prediction of flow stress in Ti–6Al–4V alloy with an equiaxed [alpha]+[beta] microstructure by artificial neural networks, *Mater. Sci. Eng. A*, 492 (2008) 276– 282.
- [20] H.Y. Li, D.D. Wei, Y.H. Li and X.F. Wang, Application of artificial neural network and constitutive equations to describe the hot compressive behavior of 28CrMnMoV steel, *Mater. Des.*, 35 (2012) 557–562.
- [21] S. Toros, F. Ozturk, Flow curve prediction of Al–Mg alloys under warm forming conditions at various strain rates by ANN, *Appl. Soft. Comput.*, 110 (2011) 1891–1898.
- [22] S. Mandal, P.V. Sivaprasad, S. Venugopal and K.P.N. Murthy, Artificial neural network modeling to evaluate and predict the deformation behavior of stainless steel type AISI 304L during hot torsion, *Appl. Soft. Comput.*, 9 (2009) 237–244.
- [23] M. Rakhshkhorshid, Modeling the hot deformation flow curves of API X65 pipeline steel, *Int. J. Adv. Manuf. Tech.*, 77 (2015) 203–210.
- [24] M. Rakhshkhorshid and A.R. Maldar, A comparative study on constitutive modeling of hot deformation flow curves in AZ91 magnesium alloy, *Iranian journal of materials Forming*, 3(1) (2016) 27–37.
- [25] M. Rakhshkhorshid and S.H. Hashemi, Experimental study of hot deformation behavior in API X65 steel, *Mater. Sci. Eng. A*, 573 (2013) 37–44.
- [26] API Specifications 5L, *Specifications for Line Pipe*, 44th Edition, American Petroleum Institute, USA (2007).
- [27] M.S. Ozerdem and S. Kolukisa, Artificial neural network approach to predict the mechanical properties of Cu–Sn–Pb–Zn–Ni cast alloys, *Mater. Des.*, 30 (2009), 764–769.

- [28] M. Zounemat-kermani, O. Kisi and T. Rajaei, Performance of radial basis and LM-feed forward artificial neural networks for predicting daily watershed run off, *Appl. Soft. Comput.*, 13 (2013) 4633– 4644.
- [29] S. Garg, S.K. Pal and D. Chakraborty, Evaluation of the performance of backpropagation and radial basis function neural networks in predicting the drill flank wear, *Neural Comput. & Applic.*, 16 (2007) pp. 407–417.
- [30] .A. Mehraei, H.R. Karimi, K.D. Thoben and B. Scholz-Reiter, Application of learning pallets for real- time scheduling by the use of radial basis function network, *Neurocomputing*, 101 (2013) 82–93.
- [31] M. Rakhshkhorshid and S.H. Hashemi, Firefly algorithm assisted optimized NN to predict the elongation of API X65 pipeline steel, *IJMMNO*, 4(3) (2013), 238 – 251.
- [32] MATLAB® software (2008) (Neural Network Toolbox, User's Guide)
- [33] H. Sarnel and Y. Senol, Accurate and robust image registration based on radial basis neural networks, *Neural Comput. & Applic.*, 20 (2011) 1255–1262.

استفاده از مدل RBF-ANN جهت پیش‌بینی منحنی‌های سیلان کار گرم فولاد API X65

مسعود رخس خورشید

گروه مکانیک، دانشکده مهندسی مکانیک و مواد، دانشگاه صنعتی بیرجند، بیرجند، ایران
بیرجند، صندوق پستی: 97175/569

چکیده: در این تحقیق، از شبکه عصبی تابع پایه شعاعی RBF-ANN جهت پیش‌بینی منحنی‌های سیلان کار گرم فولاد خط لوله API X65 استفاده شد. نتایج شبکه توسعه داده شده، با نتایج یک مدل پدیداری که اخیراً بر مبنای یک تابع توانی از پارامتر زنر-هولومون و یک تابع درجه سوم از کرنش به توان یک عدد ثابت توسعه داده شده است مقایسه گردید. از معیار ریشه میانگین مربعات خطا جهت ارزیابی عملکرد مدل‌های مورد مطالعه استفاده شد. با توجه به نتایج بدست آمده، نشان داده شد که مدل RBF-ANN عملکرد بهتری نسبت به مدل پدیداری مورد مطالعه دارد. مقدار خطای بسیار پایین 0/41 مگاپاسکال برای مدل RBF-ANN بدست آمد، که کمتر از یک-دهم خطای 4/74 بدست آمده برای معادله جامع پدیداری مورد مطالعه بود. از نتایج تحقیق حاضر می‌توان جهت شبیه‌سازی فرآیندهای شکل‌دهی گرم استفاده کرد.

کلمات کلیدی: تغییر شکل گرم، شبکه عصبی، تابع پایه شعاعی، معادلات جامع، تنش سیلان.